

*Non-Hypervascular Hypointense Nodules
at Gadoteric Acid MRI: Hepatocellular
Carcinoma Risk Assessment with Emphasis
on the Role of Diffusion-Weighted Imaging*

**Chiara Briani, Marco Di Pietropaolo,
Massimo Marignani, Francesco
Carbonetti, Paola Begini, Vincenzo
David & Elsa Iannicelli**

Journal of Gastrointestinal Cancer

ISSN 1941-6628

J Gastrointest Canc

DOI 10.1007/s12029-017-9952-7



Your article is protected by copyright and all rights are held exclusively by Springer Science +Business Media New York. This e-offprint is for personal use only and shall not be self-archived in electronic repositories. If you wish to self-archive your article, please use the accepted manuscript version for posting on your own website. You may further deposit the accepted manuscript version in any repository, provided it is only made publicly available 12 months after official publication or later and provided acknowledgement is given to the original source of publication and a link is inserted to the published article on Springer's website. The link must be accompanied by the following text: "The final publication is available at link.springer.com".

Non-Hypervascular Hypointense Nodules at Gadoteric Acid MRI: Hepatocellular Carcinoma Risk Assessment with Emphasis on the Role of Diffusion-Weighted Imaging

Chiara Briani¹ · Marco Di Pietropaolo¹ · Massimo Marignani² · Francesco Carbonetti¹ · Paola Begini² · Vincenzo David¹ · Elsa Iannicelli¹

© Springer Science+Business Media New York 2017

Abstract

Introduction and Aim In cirrhotic patients, the characterization of hypovascular nodules, hypointense on hepatobiliary phase gadoteric acid disodium-enhanced magnetic resonance images (Gd-EOB-DTPA-enhanced MRI), is essential to look for the proper approach strategy. Our objective was to evaluate the imaging features and risk assessment of hypovascular nodules, hypointense on Gd-EOB-DTPA-enhanced MRI, focusing on the diagnostic value of diffusion-weighted imaging (DWI).

Material and Methods This prospective study includes 35 patients with 50 hypovascular hypointense nodules. Signal intensity on T2-weighted images and DWI, vascular pattern on dynamic contrast-enhanced MRI and on hepatobiliary phase, and volume doubling time were analyzed for each nodule as well as patient's clinical features. Univariate and multivariate analyses were made to determine the variables associated with the development of hypervascular pattern.

Results On 24 months follow-up period, 40% of the hypointense nodules (mean size 14 mm ± 6.1) became hypervascular hepatocellular carcinoma (HCC) with 6 and 12 months cumulative risk of 45 and 55%. Nine/12 (75%, mean size 15.50 mm ± 7.2) that appeared hyperintense in DWI at first exam show malignant transformation (p value = 0.007). Univariate and multivariate analyses identified hyperintensity at initial DWI (OR 6.49; 95% CI 1.28–32.80; p

value = 0.009) and size ≥ 10 mm (OR 6.22; 95% CI 1.57–24.63; p value = 0.024) as independent factors with the development of HCC.

Conclusion In conclusion, hypovascular lesions ≥ 10 mm and those hyperintense in DWI were associated with progression to hypervascular HCC. A close follow-up or histological characterization is recommended to improve patients outcome and to develop effective treatment.

Keywords Hepatocarcinogenesis · MR imaging · Liver cirrhosis · Diffusion-weighted imaging · Hepatocellular carcinoma

Introduction

Hepatocellular carcinoma (HCC) is one of the most common malignancies in the world and the major cause of cancer-related mortality in patients with cirrhosis. Epidemiological data show a progressive increase in incidence in industrialized countries, with about 749,000 new cases diagnosed annually and 695,000 deaths per year from liver cancer [1].

The early detection and characterization of focal liver lesions is critical for optimal patient management [2, 3]. The treatment options are based mainly on the stage when the tumor is first diagnosed: the change for curative therapies, including liver transplantation (according to Milan criteria), liver resection, or local-regional treatment increases the patient survival rate and offers the best chance for long-term survival with a 5-year survival rate approaching 75% [4, 5].

Hepatocellular carcinoma develop by a multistep process arise from regenerative to dysplastic nodule (DN) (low grade-high grade), then to well-differentiated HCC, and finally evolves into advanced hypervascular HCC characterized by

✉ Chiara Briani
chiara.briani@uniroma1.it

¹ Radiology Unit, Sapienza University of Rome, Sant'Andrea Hospital, Rome, Italy

² Department of Digestive and Liver Disease, Sapienza University of Rome, Sant'Andrea Hospital, Rome, Italy

intense vascularization after the recruitment of an arterial blood supply by the hepatic artery [6].

According to the guidelines of the American Association for the Study of Liver Disease (AASLD) [4], the diagnosis of HCC in cirrhotic patients, with a lesion ≥ 1 cm is established on enhanced computed tomography or magnetic resonance imaging (MRI), showing the typical pattern of hypervascular in the arterial phase and washout in the portal phase and late without biopsy confirmation [4].

Unfortunately, hypovascular well-differentiated HCCs, early HCC or DNAs, may present atypical features on dynamic study, due to the lack of the typical hemodynamic changes, showing hypovascularity on arterial phase images.

Gadoxetic acid disodium (Gd-EOB-DTPA) offers the combined properties of an extracellular space contrast agent during the vascular-interstitial phases and liver-specific magnetic resonance contrast agent allowing evaluation of hepatocyte uptake with subsequent biliary excretion assessing the metabolic function of nodules which can help the characterization and detection of hypovascular HCC and their precursors.

Diffusion-weighted imaging (DWI) seems to show a good efficiency in identifying lesions, according to the quantitative evaluation of the molecular motion, depending on the microstructural organization of the district examined [7]. In tumors structures, cell density substantially increases with a decrease in the extracellular space. This results in a subsequent decrease in mobility, which leads to restricted diffusion [8].

The combination of Gd-EOB-DTPA and DWI could allow assessment of three processes of hepatic multistep carcinogenesis (vascular changes, hepatocyte change, and tissue diffusivity).

Therefore, in a context where characterization of hypovascular nodules remains complicated [9] and their management is still a contentious issue, we conducted this study with the aim to investigate the imaging features and the natural outcome of hypovascular nodules, hypointense on hepatobiliary phase gadoxetic acid-enhanced magnetic resonance images (Gd-EOB-DTPA-enhanced MRI), focusing on the diagnostic value of DWI, to look for a better approach strategy.

Material and Methods

Study Group

We conducted a prospective longitudinal study, between January 2014 and February 2017, on patients with chronic liver disease who showed hypointense nodule on hepatobiliary phase Gd-EOB-DTPA-enhanced MRI, performed for surveillance program or follow-up for treated HCC.

The following inclusion criteria were used: (1) hypointense lesions on hepatobiliary phase without hypervascularization on arterial phase images and (2) available of 3 months Gd-EOB-DTPA-enhanced MRI including DWI sequences, for at least 24 months.

The exclusion criteria were as follows: (1) patients with hemosiderosis and hemochromatosis and (2) portal vein thrombosis, serious renal failure, or previous adverse reactions to gadolinium contrast agent. Therefore, 35 patients with 50 nodules were enrolled in the study (Table 1).

The final diagnosis of HCC was made according to the guidelines from the AASLD [4]. We analyzed the clinical data for determine the clinical features associated with the development of hypervascular pattern.

This study was approved by the Institutional Review Board of our hospital and written informed consent was obtained from each patient.

MRI Protocol

Magnetic resonance imaging was performed using a 1.5-T scanner (Sonata Siemens, Erlangen, Germany), with element phased-array surface body coil. The detailed parameters are shown in Table 2.

DWI was acquired with echo-planar imaging sequence (b values 50–400–800 s/mm^2) with respiratory triggering. An apparent diffusion coefficient (ADC) maps was derived on a voxel-by-voxel basis by using a commercial software.

Table 1 Characteristics of patients ($N = 35$)

Variables	Values
Age (years) \pm SD	Mean 68 \pm 8.6
Gender (male-female)	26 (74%):9 (26%)
Etiology	
• HCV	21 (60%)
• HBV	9 (25%)
• Cryptogenic	2 (6%)
• Alcohol	2 (6%)
• Primary biliary cirrhosis	1 (3%)
Height (m) \pm SD	Mean 1.72 \pm 0.06
Weight (kg) \pm SD	Mean 81.22 \pm 2.33
BMI (kg/m^2) \pm SD	Mean 16.77 \pm 1.22
Child-Pugh class	
A	28 (80%)
B	7 (20%)
AFP	
<20 ng/mL	20 (57%)
20–200 ng/mL	10 (29%)
>200 ng/mL	5 (14%)

SD standard deviation, HBV hepatitis B virus, HCV hepatitis C virus, BMI body mass index, AFP α -fetoprotein

Table 2 Magnetic resonance parameters

	DWI MRI	T2WI	T1WI	DCE MRI
Sequence	Single-shot dual spin-echo EPI	Turbo spin-echo	Fast gradient echo	Gradient echo with 3D acquisition (VIBE)
Matrix	128	320	256	256
Acquisition time	3 min	20 s	31 s ^a	18 s
TE (ms)	68	119	2.4 and 4.5	1.8
TR (ms)	2900	2000–3000	125	4.5
Flip angle (degrees)	90	180	70	10
Slice thickness (mm)	5	6	5	3
Fat saturated	–	Yes	–	Yes
Respiratory triggered	Yes	Yes	–	–
Other	<i>b</i> values of 50–400–800 s/mm ²			Scan delay after administration: 30–35 s, 70–80 s, 180 s, 20 min

DWI diffusion-weighted imaging, MRI magnetic resonance imaging, DCE MRI dynamic contrast-enhanced MRI, EPI echo-planar imaging, VIBE volumetric interpolated breath-hold examinations, TE echo time, TR repetition time

^a Two breath holds were required in many cases

Three-dimensional volumetric interpolated breath-hold examinations were acquired before and after intravenous bolus injection of Gd-EOB-DTPA (0.025 mmol/kg of body weight) at a rate of 0.8–1 ml/s, followed by a 10-cm³ saline flush at the same injection rate. For Gd-EOB-DTPA-enhanced MRI arterial phase (30–35 s), portal phase (70–80 s) and equilibrium phase images (180 s) were obtained following the contrast agent injection.

The time for the arterial phase imaging was determined by using the magnetic resonance bolus detection technique. Hepatobiliary phase images were acquired with a delay of 20 min after injection, by using volumetric interpolated breath-hold examinations sequence (axial and coronal planes) and fast low-angle shot 2D T1 fat-sat high-resolution sequence.

Image Analysis

Magnetic resonance images were interpreted by two abdominal radiologists in consensus with 20 and 10 years of experience in liver MRI, respectively.

The parameters evaluated included the nodule size, the signal intensity on unenhanced T2-weighted images and on hepatobiliary phase images, as well as the lesion's vascular pattern on dynamic contrast-enhanced MRI, the presence of hyperintensity on high *b* value DWI (*b* = 800 s/mm²) and ADC values on ADC maps.

The signal intensity (SI) of the lesions was measured before the injection of the contrast agent and 20 min after the injection of Gd-EOB-DTPA in T1-weighted images with fat suppression. The SI of the lesions was calculated by setting a circular region of interest. Relative enhancement was calculated with the following formula: RE = (SI (after enhancement) – SI (before enhancement))/SI (before enhancement).

The lesion size was calculated as the longest diameters of the nodules in the axial plane on hepatobiliary phase image. For nodules enlarged during follow-up, lesions were re-measured on the last follow-up MRI; thereafter, the tumor volume doubling time was calculated based on the Schwartz formula [10].

$$DT = \frac{(T2-T1)\ln 2}{\ln \left(\frac{V2}{V1} \right)}$$

where V1 and V2 are two tumor volume estimates at two different time, at the initial MRI and at the last follow-up MRI, respectively.

On DWI, a lesion was defined as hyperintense only when it showed hyperintensity at *b* = 800 s/mm² compared to the signal drop of background parenchyma with equivalent or a lower ADC value compared to the background parenchyma on the ADC map.

A lesion was defined as hypovascular nodule when it was hypointensity on hepatobiliary phase and no hypervascularity on arterial phase images. Lesion was considered as definitely being HCC when it was larger than 10 mm showing the typical vascular pattern for HCC according to the AASLD criteria [4].

Statistical Analysis

Fisher's exact test or the chi-square test, when needed, was used to evaluate the relationship between individual parameters and evolution. The Student's *t* test was used to compare the average age between the two groups (evolved vs. non-evolved) and the Mann-Whitney test was used to compare

alpha fetoprotein distribution and number of treatments between the two groups.

The test for trend was used to evaluate the trend of the variable presence of HCC between the two groups. The odds ratio and their 95% confidence intervals (95% CI) were calculated for each factor, using univariate logistic regression.

The factors with a univariate association with p value <0.1 were included in the stepwise multivariate model (output probability 0.1). The OR adjusted (OR adj) and its confidence intervals were calculated for the two factors remaining in the model. A p value <0.05 was considered to indicate statistically significant differences.

The statistical analysis was performed by using a statistical software (Systat Software, Inc. Sigma Plot for Windows version 12.0).

Results

A total of 35 patients with 50 hypointense nodules (mean size $11.7 \text{ mm} \pm 5.5$) were enrolled in the study (Figs. 1a, b, 2a, b,

and 3a, b). Twelve/50 (24%) nodules showed hyperintensity on DWI (mean size $15 \text{ mm} \pm 6.9$) (Fig. 1c) with a mean ADC values of $1.10 \times 10^{-3} \text{ m}^2/\text{s} \pm 0.33$.

During 24 months follow-up period, arterial hypervascularization was observed in 40% of the hypointense nodules (20/50, mean size $14 \text{ mm} \pm 6.1$) that show a typical vascular pattern of HCC (Figs. 1 and 2).

Fifteen/20 lesions were $\geq 10 \text{ mm}$ (mean size $16.2 \text{ mm} \pm 5.6$) at the first exam; the others five nodules (mean size $7.6 \text{ mm} \pm 0.8$) have increased in size ($>1 \text{ cm}$) during the follow-up period.

The estimated 6 and 12 months cumulative risk of nodule hypervascularization were 45 and 55%, respectively.

The remaining 30 nodules did not show hypervascularization on arterial phase images during the 24 months follow-up (mean size $9.5 \text{ mm} \pm 4.2$) (Fig. 3). The tumor volume doubling time in the hypervascular group was shorter than that in the non-hypervascular group, with a mean of 772 vs. 1179 days, respectively.

Univariate analysis shows significant differences between the nodules with and without hypervascular transformation

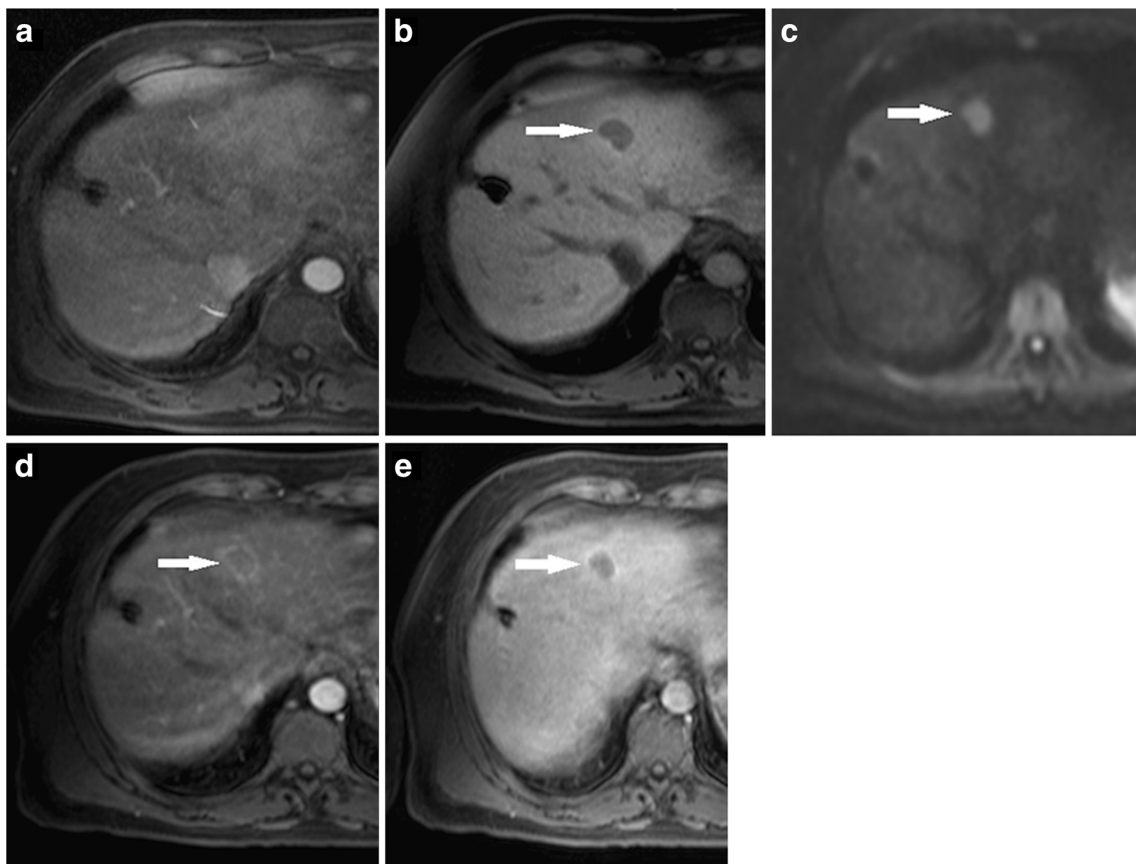


Fig. 1 MR images of hepatocellular nodule that progress to hypervascular HCC in a 71-year-old man. Axial gadoxetic acid-enhanced arterial phase image does not show hypervascular focal liver lesions (a). The hepatobiliary phase image shows a hypointense nodule (arrow) (b) with hyperintensity on DWI at $800 \text{ s}/\text{mm}^2$ (arrow) (c). After

12 months follow-up period, the lesion shows enhancement on arterial phase (arrow) (d) and washout on equilibrium phase images (arrow) (e). The histological result confirmed the diagnosis of hepatocellular carcinoma

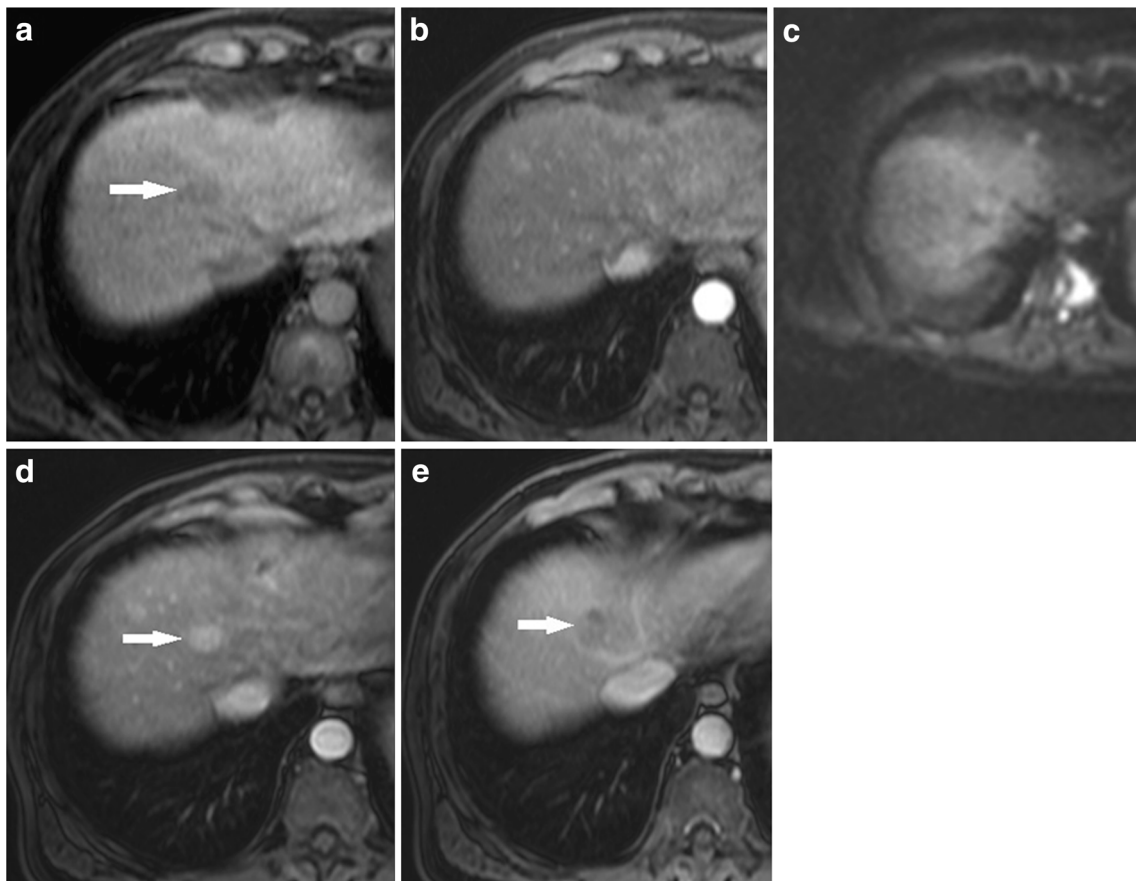


Fig. 2 MR images of hepatocellular nodule that progress to hypervascular HCC in a 68-year-old woman with hepatitis C virus-related cirrhosis (**a**). Axial gadoxetic acid-enhanced 20-min HBP image demonstrates a hypointense nodule (*arrow*) not showing arterial enhancement in arterial phase image (**b**). Axial single-shot echo-planar

DW image (**b** 800 s/mm²) does not detect liver nodule (**c**). Six months later, during the follow-up, dynamic MR images show a typical vascular pattern of HCC: hypervascularity on the arterial phase image (*arrow*) (**d**) and washout in the equilibrium phase image (*arrow*) (**e**)

with regard to nodule's size (≥ 10 mm, p value = 0.002) and hyperintensity at initial DWI. Nine/12 (75%, mean size 15.5 mm \pm 7.2) that appeared hyperintense in DWI at the first exam show malignant transformation (p value = 0.007) (Fig. 1).

The mean ADC values of the transformer group was lower than that in the “stable” group (1.03×10^{-3} m²/s \pm 0.28 vs. 1.27×10^{-3} m²/s \pm 0.30), although the difference was not statistically significant (p value > 0.05). No significant differences in other evaluation items were observed.

In addition, multivariate analysis confirmed that hyperintensity on DWI (OR 6.49; 95% CI 1.28–32.80; p value = 0.009) and size ≥ 10 mm (OR 6.22; 95% CI 1.57–24.63; p value = 0.024) are independently associated with the development of HCC.

An increase of value of alpha fetoprotein increases the risk of evolution (OR 1008; 95% CI 1.002–1.013; p value = 0.009), although is not related as independent factors for hypervascular transformation (p value = 0.072). The results of analysis are summarized in Tables 3 and 4.

Discussion

Magnetic resonance imaging plays a crucial role in the management of patients with liver cirrhosis, but dynamic images sometimes provide inconclusive findings in the detection and characterization of liver lesions.

Technological and protocol advancements with liver-specific contrast agents makes a positive impact in patient management strategies in clinical practice [11–15]. Recent studies [12, 16–18] have demonstrated that Gd-EOB-DTPA is uptaken by means of organic-anion transporting polypeptide, and the decrease of their expression, and therefore the Gd-EOB-DTPA uptake, precedes the reduction of portal blood flow and neoangiogenesis.

Therefore, hypointensity on hepatocyte phase well correlated with the initial phase of carcinogenesis.

Almost all nodules included in this study were equal or less than 2 cm in size (96%) and they could be considered “small HCC” by the definition of the International Working Party of the World Congress of Gastroenterology in 1995 [19]. In 2009, the International Consensus Group for Hepatocellular

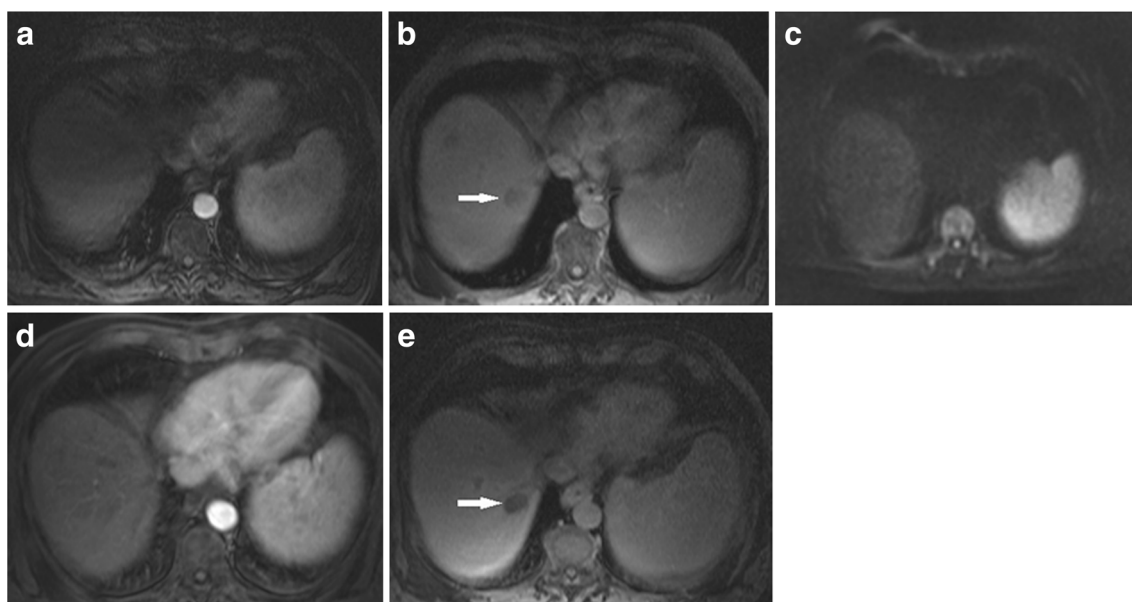


Fig. 3 MR images of hepatocellular nodule that did not progress to hypervascular HCC in a 65-year-old man with hepatitis B virus-related cirrhosis. No focal lesions are detected on arterial phase image (a). HBP image shows a hypointense lesion (arrow) (b) that does not show

hyperintensity on axial single-shot echo-planar DW image at **b** 800 s/mm^2 (c). After 6 months, no evidence of enhancing lesion on arterial phase image (d) and the lesion is clearly hypointense on HBP image (arrow) (e)

neoplasia [6] referred early HCCs to as “small HCC of the vaguely nodular type.” Early HCCs are considered “in situ carcinoma” showing well-differentiated proliferation [12] with the development of unpaired arteries.

Most of these nodules are still hypovascular on dynamic MRI, only 5% of the early HCCs show arterial hypervascularity on dynamic contrast-enhanced MRI [20]. Nodules at this stage have a high chance of surgical cure, lower recurrence rates, and more favorable outcome [21–23] with a surgical resection survival rate and recurrence-free survival rate at 5 years of 93 and 47%, respectively [24].

Gd-EOB-DTPA-enhanced MRI is used to combine functional and morphological analysis and could allow the detection of iso-hypovascular pre-malignant (low-grade DNs-high-grade DNs) and malignant (early HCCs-hypovascular HCCs) lesions [12, 25–27].

In our study 40% of hypointense nodules of Gd-EOB-DTPA developed hypervascularization and an increased size, showing the typical vascular pattern for HCC according to AASLD criteria [4], with a cumulative risk of hypervascularization of 6 months of 45% and 12 months of 55%.

Our results are consistent with other studies [28–30] and highlight the role of close follow-up to early detection and characterization of hypovascular nodules that can potentially progress to hypervascular HCC.

In addition, it is interesting to know that, as suggested by Komatsu et al. [31], the presence of hypointense nodules appears to be associated with a higher risk for developing HCC not only at the same site from initial nodule but also at any sites of the liver.

Our results, displayed in Tables 3 and 4, show that hyperintensity in DWI at first exam and lesion size are the only variables significantly correlated with hypervascular transformation, identifying them as independent factors in predicting malignant transformation in multivariate analysis.

None of the clinical findings included serum alpha fetoprotein level, etiology, comorbidity, Child-Pugh class, and coexistence of hypervascular HCC show correlation with arterialization in hepatobiliary phase hypointense nodules on follow-up.

In our study 75% of hypointense nodules that appeared hyperintense in DWI at first exam show malignant transformation (p value = 0.007) (Fig. 1). On the other hand, in our experience, hyperintensity detected in T2-weighted images are not significantly predictive of malignancy (p value = 0.065).

In the multistep pathway of hepatocarcinogenesis, several cellular changes occur, including an increase of cell density, with a consequent decreased thickness of extracellular space and an increase of both nuclear-to-cytoplasmic ratio and thickening of cellular plates.

All these mechanisms lead to a reduction of mobility of water molecules that results in a restricted diffusion detectable through DWI [8].

As reported in other studies [32–34], adding DWI to dynamic contrast-enhanced MRI can improve the diagnostic accuracy in the diagnosis of hepatic nodules and to predict the outcome of hypointense nodules in the hepatobiliary phase.

Moreover, to provide a quantitative index of diffusion, quantitative ADC measured was also performed. We found a

Table 3 Evolution of hypointense nodules on hepatobiliary phase: characteristics of patients

Variables	Hypervascularization		<i>p</i> value- <i>U</i>
	Yes (<i>n</i> : 20)	No (<i>n</i> : 30)	
Age (years) ± SD	62.2 ± 8.5	62.6 ± 10.4	0.900
Serum AFP level (ng/mL) ± SD	38 ± 12.5	15 ± 6.5	0.072
Etiology			0.345
HCV	14 (47%)	16 (53%)	
HBV	3 (43%)	4 (57%)	
Non-B; non-C	3 (23%)	10 (77%)	
Comorbidity			0.180
Yes	22 (67%)	11 (33%)	
No	9 (53%)	8 (47%)	
Child-Pugh class			0.130
A	14 (35%)	26 (65%)	
B	6 (60%)	4 (40%)	
Coexistence of hypervascular HCC			0.078
Yes	18 (43%)	24 (57%)	
No	2 (25%)	6 (75%)	
Previous history of HCC ± SD	4 ± 0.2	3 ± 0.8	0.131

N (%) or mean, *SD* standard deviation, *HBV* hepatitis B virus, *HCV* hepatitis C virus, *AFP* α-fetoprotein, *p* value-*U* univariate analysis, *Previous history of HCC* number of treated HCC before the enrollment into the study

tendency toward a lower mean ADC in the transformer group than the stable group; nevertheless, no significant difference was found (*p* value > 0.05).

The typical architecture of cirrhotic liver is characterized by an increasing of fibrotic tissue and a consequent decreased blood flow therefore the ADC value takes into account also perfusion random motions that occur in the capillary network [35]. Furthermore, cirrhotic parenchyma and solid benign lesions have low ADC values that will lead to a considerable overlap with malignant lesions [36, 37]. The role of ADC evaluation is still controversial and the lack of international standardization for the *b* value setting does not allow obtaining comparable results.

Our results highlight that the incidence of hypervascularization is significantly higher for nodules ≥10 mm in size (*p* value = 0.002) with a tumor volume doubling time shorter than that of the stable group with a mean of 772 vs. 1179 days, respectively.

In this context, we are in agreement with the Consensus-Based Clinical Practice Guidelines proposed by the Japan Society of Hepatology [38] that underline the important role of gadoxetic acid in the evaluation of atypical vascular pattern lesions, including Gd-EOB-DTPA in the diagnostic and treatment algorithms for hypovascular nodules, and recommended biopsy of hypointense nodules of 1–1.5 cm or larger for differential diagnosis between early HCC and DN.

Table 4 Evolution of hypointense nodules on hepatobiliary phase: magnetic resonance imaging findings

Variables	Hypervascularization		<i>p</i> value- <i>U</i>	<i>p</i> value- <i>M</i>	Odds ratio (95% CI)
	Yes (<i>n</i> : 20)	No (<i>n</i> : 30)			
Mean size mm (±SD)	14 mm (±6.1)	9.5 mm (±4.2)	0.002		
Nodules ≥ 10 mm in size at the first exam	15 (62%)	9 (38%)	0.002	0.024	6.22 (1.57–24.63)
T2-weighted images			0.065		
Hyperintense	8 (61%)	5 (39%)			
Isointense	12 (32%)	25 (68%)			
DW imaging			0.007	0.009	6.49 (1.28–32.80)
Hyperintense	9 (75%)	3 (25%)			
Isointense	11 (29%)	27 (71%)			

SD standard deviation, *DW* diffusion weighted, *p* value-*U* univariate analysis, *p* value-*M* multivariate analysis, 95% CI 95% confidence intervals

In our opinion modify the current clinical practice following this guidelines could be worthwhile.

A previous study reported that the only independent associated factor for arterial hypervascularization of hypointense nodule of hepatobiliary phase is hyperintensity either on T2-weighted images [30] or on DWI [29].

The main strength of our study is that two imaging features, hyperintensity on DWI and nodules size, appear to be compelling predictive marker independently associated with an increased risk of hypervascular transformation.

We believe that our results allow a deep knowledge of the significant of non-hypervascular hypointense nodules and of the role of imaging in predict the malignant transformation and characterization of liver lesions: nodules that show hyperintensity on DWI and size ≥ 10 mm with faster growth may be more frequent follow-up and biopsy is recommended in order to differentiate early HCC from DNs and to develop effective treatment [39].

Following this opinion Kim et al. [23] conclude that percutaneous radiofrequency ablation is effective for treating both high-grade DNs and well-differentiated HCCs.

Matsuda et al. [39] show that preoperative Gd-EOB-DTPA-enhanced MRI and simultaneous treatment of early HCC prolonged recurrence-free survival after hepatic resection with a 5-year recurrence-free survival rates of 48.7 versus 25.5% (p value < 0.01).

Furthermore, the attractive of this result is that the lack of significant correlation between clinical findings and the hypervascular transformation strengthens the role of imaging in predicting the malignant transformation among hepatobiliary phase hypointense nodules.

Our results point out that imaging can stratify patient for clinical purpose. Imaging is a useful tool in the management of cirrhotic patients improving and allowing selection of patients that required close follow-up and that can be followed by ambulatory care with better quality and effectiveness of care in the health system.

Our study has some limitations: (1) the small sample size and (2) the lack of the histopathological confirmation not allowing the analysis of correlation between imaging of hypointense nodules and their histological findings. Nevertheless, this was not the purpose of our study because our main goal was to assess the correlation between imaging findings and patient outcome.

In conclusion, our study highlights the high risk of hypointense nodules on hepatobiliary phases of malignant transformation. Even more interesting is the demonstration that hypovascular lesions ≥ 10 mm and those that appeared hyperintense in DWI were associated with progression to hypervascular HCC.

Therefore, in these cases, a close follow-up is recommended to improve patient's outcome.

Some studies confirm the possibility of treating HCC at an early stage [23, 39, 40], and Gd-EOB-DTPA-enhanced MRI associated with DWI could allow a more efficient and early selection of nodules that could be treated effectively at an early stage.

Compliance with Ethical Standards

Conflict of Interest The authors declare that they have no conflict of interest.

Ethical Approval All procedures performed in studies involving human participants were in accordance with the ethical standards of the institutional and/or national research committee and with 1964 Helsinki declaration and its later amendments or comparable ethical standards.

References

1. Globocan (2008), Cancer data sheet. Cited 11th December 2012. <http://globocan.iarc.fr/factsheets/cancers/liver.asp>.
2. Al Hasani F, Knoepfli M, Gemperli A, Kollar A, Banza V, Kettenbach J, et al. Factors affecting screening for hepatocellular carcinoma. *Ann Hepatol*. 2014;13:204–10.
3. Gaba RC, Kallwitz ER, Parvinian A, Bui JT, Von Roenn NM, Berkes JL, et al. Imaging surveillance and multidisciplinary review improves curative therapy access and survival in HCC patients. *Ann Hepatol*. 2013;12:766–73.
4. Bruix J, Sherman M, American Association for the Study of Liver Disease. Management of hepatocellular carcinoma: an update. *Hepatology*. 2011;53:1020–2. doi:10.1002/hep.24199.
5. Memeo R, De Blasi V, Cherkaoui Z, Dehlawi A, De'Angelis N, Piardi T, et al. New approaches in locoregional therapies for hepatocellular carcinoma. *J Gastrointest Cancer*. 2016;47(3):239–46. doi:10.1007/s12029-016-9840-6.
6. International Consensus Group for Hepatocellular Neoplasia. Pathologic diagnosis of early hepatocellular carcinoma: a report of the International Consensus Group for Hepatocellular Neoplasia. *Hepatology*. 2009;49:658–64. doi:10.1002/hep.22709.
7. Taouli B, Koh DM. Diffusion-weighted MR imaging of the liver. *Radiology*. 2010;254:47–66. doi:10.1148/radiol.09090021.
8. Culverwell AD, Sheridan MB, Guthrie JA, Scarsbrook AF. Diffusion-weighted MRI of the liver—interpretative pearls and pitfalls. *Clin Radiol*. 2013;68:406–14. doi:10.1016/j.crad.2012.08.008.
9. Arii S, Sata M, Sakamoto M, Shimada M, Kumada T, Shiina S, et al. Management of hepatocellular carcinoma: report of consensus meeting in the 45th Annual Meeting of the Japan Society of Hepatology. *Hepatol Res*. 2010;40:667–85. doi:10.1111/j.1872-034X.2010.00673.
10. Schwartz M. A biomathematical approach to clinical tumor growth. *Cancer*. 1961;14:1272–94.
11. Van Beers BE, Pastor CM, Hussain HK. Primovisteovist: what to expect? *J Hepatol*. 2012;57:421–9. doi:10.1016/j.jhep.2012.01.031.
12. Park YN. Update on precursor and early lesions of hepatocellular carcinomas. *Arch Pathol Lab Med*. 2011;135:704–15. doi:10.1043/2010-0524-RA.1.
13. Silva AC, Evans JM, McCullough AE, Jatoti MA, Vargas HE, Hara AK. MR imaging of hypervascular liver masses: a review of current techniques. *Radiographics*. 2009;29:385–402. doi:10.1148/rg.292085123.

14. Di Pietropaolo M, Briani C, Pillozzi E, Carbonetti F, David V, Iannicelli E. Gd-EOB-DTPA-enhanced magnetic resonance findings of a giant inflammatory hepatocellular adenoma: a case report and review of the literature. *J Gastrointest Cancer*. 2015;46:421–5. doi:10.1007/s12029-015-9715-2.
15. Imura S, Shimada M, Utsunomiya T. Recent advances in estimating hepatic functional reserve in patients with chronic liver damage. *Hepatol Res*. 2015;45:10–9. doi:10.1111/hepr.12325.
16. Narita M, Hatano E, Arizono S, Miyagawa-Hayashino A, Isoda H, Kitamura K, et al. Expression of AOTF1B3 determines uptake of Gd-EOB-DTPA in hepatocellular carcinoma. *J Gastroenterol*. 2009;44:793–8. doi:10.1007/s00535-009-0056-4.
17. Kitao A, Matsui O, Yoneda N, Kozaka K, Shinmura R, Koda W, et al. The uptake transporter OATP8 expression decreases during multistep hepatocarcinogenesis: correlation with gadolinium-enhanced MR imaging. *Eur Radiol*. 2011;21:2056–66. doi:10.1007/s00330-011-2165-8.
18. Kogita S, Imai Y, Okada M, Kim T, Onishi H, Takamura M, et al. Gd-EOB-DTPA-enhanced magnetic resonance images of hepatocellular carcinoma: correlation with histological grading and portal blood flow. *Eur Radiol*. 2010;20:2405–13. doi:10.1007/s00330-010-1812-9.
19. International Working Party. Terminology of nodular hepatocellular lesions. *Hepatology*. 1995;22:983–93.
20. Huh J, Kim KW, Kim J, Yu E. Pathology-MRI correlation of hepatocarcinogenesis: recent update. *J Pathol Transl Med*. 2015;49:218–29. doi:10.4132/jptm.2015.04.15.
21. Lee DH, Lee JM, Lee JY, Kim SH, Kim JH, Yoon JH, et al. Non hypervascular hepatobiliary phase hypointense nodules on gadolinium-enhanced MRI: risk of HCC recurrence after radiofrequency ablation. *J Hepatol*. 2015;62:1122–30. doi:10.1016/j.jhep.2014.12.015.
22. Kurokohchi K, Deguchi A, Masaki T, Himoto T, Yoneyama H, Kobayashi M, et al. Successful treatment of hypovascular advanced hepatocellular carcinoma with lipiodol-targeting intervention radiology. *World J Gastroenterol*. 2007;13:4398–400.
23. Kim SH, Lim HK, Kim MJ, Choi D, Rhim H, Park CK. Radiofrequency ablation of high-grade dysplastic nodules in chronic liver disease: comparison with well-differentiated hepatocellular carcinoma based on long-term results. *Eur Radiol*. 2008;18:814–21.
24. Takayama T, Makuuchi M, Hirohashi S, Sakamoto M, Yamamoto J, Shimada K, et al. Early hepatocellular carcinoma as an entity with a high rate of surgical cure. *Hepatology*. 1998;28:1241–6.
25. Bartolozzi C, Battaglia V, Bargellini I, Bozzi E, Campani D, Pollina LE, et al. Contrast-enhanced magnetic resonance imaging in 102 nodules in cirrhosis: correlation with histological findings on explanted livers. *Abdom Imaging*. 2013;38:290–6. doi:10.1007/s00261-012-9952-9.
26. Iannicelli E, Di Pietropaolo M, Marignani M, Briani C, Federici GF, DelleFave G, et al. Gadolinium-enhanced MRI for hepatocellular carcinoma and hypointense nodule observed in the hepatobiliary phase. *Radiol Med*. 2014;119:367–76. doi:10.1007/s11547-013-0364-x.
27. Jang KM, Kim SH, Kim YK, Choi D. Imaging features of subcentimeter hypointense nodules in gadolinium-enhanced hepatobiliary phase MR imaging that progress to hypervascular hepatocellular carcinoma in patients with chronic liver disease. *Acta Radiol*. 2015;56:526–35. doi:10.1177/0284185114534652.
28. Inoue T, Hyodo T, Murakami T, Takayama Y, Nishie A, Higaki A, et al. Hypovascular hepatic nodules showing hypointense on the hepatobiliary-phase image of Gd-EOB-DTPA-enhanced MRI to develop a hypervascular hepatocellular carcinoma: a nationwide retrospective study on their natural course and risk factors. *Dig Dis*. 2013;31:472–9. doi:10.1159/000355248.
29. Kim YK, Lee WJ, Park MJ, Kim SH, Rhim H, Choi D. Hypovascular hypointense nodules in hepatobiliary phase gadolinium-enhanced MR images in patients with cirrhosis: potential of DWI imaging in predicting progression to hypervascular HCC. *Radiology*. 2012;265:104–14.
30. Hyodo T, Murakami T, Imai Y, Okada M, Hori M, Kagawa Y, et al. Hypovascular nodules in patients with chronic liver disease: risk factors for development of hypervascular hepatocellular carcinoma. *Radiology*. 2013;266:480–90. doi:10.1148/radiol.12112677.
31. Komatsu N, Motosugi U, Maekawa S, Shindo K, Sakamoto M, Sato M, et al. Hepatocellular carcinoma risk assessment using gadolinium-enhanced hepatocyte phase magnetic resonance imaging. *Hepatol Res*. 2014;44:1339–46. doi:10.1111/hepr.12309.
32. Park MJ, Kim YK, Lee MW, Lee WJ, Kim YS, Kim SH, et al. Small hepatocellular carcinomas: improved sensitivity by combining gadolinium-enhanced and diffusion-weighted MR imaging patterns. *Radiology*. 2012;264:761–70. doi:10.1148/radiol.12112517.
33. Piana G, Trinquart L, Meskine N, Barrau V, Beers BV, Vilgrain V. New MR imaging criteria with a diffusion-weighted sequence for the diagnosis of hepatocellular carcinoma in chronic liver diseases. *J Hepatol*. 2011;55:126–32. doi:10.1016/j.jhep.2010.10.023.
34. Park MJ, Kim YK, Lee MH, Lee JH. Validation of diagnostic criteria using gadolinium-enhanced and diffusion-weighted MR imaging for small hepatocellular carcinoma (<= 2.0 cm) in patients with hepatitis-induced liver cirrhosis. *Acta Radiol*. 2013;54:127–36. doi:10.1258/ar.2012.120262.
35. Girometti R, Furlan A, Esposito G, Bazzocchi M, Como G, Soldano F, et al. Relevance of b-values in evaluating liver fibrosis: a study in healthy and cirrhotic subjects using two single-shot spin-echo echo-planar diffusion-weighted sequences. *J Magn Reson Imaging*. 2008;28:411–9. doi:10.1002/jmri.21461.
36. Taouli B, Vilgrain V, Dumont E, Daire JL, Fan B, Menu Y. Evaluation of liver diffusion isotropy and characterization of focal hepatic lesions with two single-shot echo-planar MR imaging sequences: prospective study in 66 patients. *Radiology*. 2003;226:71–8.
37. Lee MH, Kim SH, Park MJ, Park CK, Rhim H. Gadolinium-enhanced hepatobiliary phase MRI and high b-value diffusion-weighted imaging to distinguish well-differentiated hepatocellular carcinomas from benign nodules in patients with chronic liver disease. *AJR Am J Roentgenol*. 2011;97:868–75. doi:10.2214/AJR.10.6237.
38. Kudo M, Matsui O, Izumi N, Lijima H, Kadoya M, Imai Y, et al. JSH Consensus-Based Clinical Practice Guidelines for the Management of Hepatocellular Carcinoma: 2014 Update by the Liver Cancer Study Group of Japan. *Liver Cancer*. 2014;3:458–68. doi:10.1159/000343875.
39. Matsuda M, Ichikawa T, Amemiya H, Maki A, Watanabe M, Kawaida H, et al. Preoperative gadolinium-enhanced MRI and simultaneous treatment of early hepatocellular carcinoma prolonged recurrence-free survival of progressed hepatocellular carcinoma patients after hepatic resection. *HPB Surg*. 2014;64:1685 doi:10.1155/2014/641685.
40. Nathan H, Hyder O, Mayo SC, Hirose K, Wolfgang CL, Chiti MA, et al. Surgical therapy for early hepatocellular carcinoma in the modern era: a 10-year SEER-medicare analysis. *Ann Surg*. 2013;258:1022–7. doi:10.1097/SLA.0b013e31827da749.